

PACS numbers: 42.25.Dd; 42.25.Fx; 42.65.Re
DOI: 10.1070/QE2006v036n11ABEH013332

Propagation of a femtosecond pulse in a scattering medium: theoretical analysis and numerical simulation

E.A. Sergeeva, M.Yu. Kirillin, A.V. Priezzhev

***Abstract*. The time profile of a femtosecond pulse propagating in media with a high scattering anisotropy ($g \geqslant 0.9$) is studied in detail. The iteration method based on the expansion of the light field in a series in photon scattering orders with the account for the multiply scattered component is proposed to study analytically the structure of a scattered radiation pulse. The small-angle approximation of the radiation transfer theory used for calculations of low-order scatterings is modified to take into account the spread in the photon delay times. The shape of a scattered ultrashort pulse calculated theoretically well agrees with the shape obtained by the Monte-Carlo simulation. It is shown that the pulse profile in a scattering medium depends on the shape of the scattering phase function with the conservation of the anisotropy factor. A comparative analysis of contributions from different scattering orders to the pulse structure is performed depending on the optical properties of a scattering medium.**

Keywords: *femtosecond pulse, multiple light scattering, radiation transfer theory, small-angle approximation, numerical simulation, Monte-Carlo method.*

1. Introduction

The study of propagation of femtosecond pulses in a scattering medium is of current interest due to the development of optical methods for diagnostics of biological tissues with a submicron resolution. Modern compact femtosecond lasers tunable in the visible and IR spectral regions are used in optical coherence tomography (OCT) [1 – 3] and multiphoton fluorescence microscopy (MFM) [2, 3]. However, the application of these methods for detailed visualisation of the structure of biological tissues at depths exceeding one millimetre is restricted by a strong spreading of an ultrashort pulse due to scattering in the tissue resulting in the impairment of resolution over the penetration depth and a decrease in the peak power of the pulse.

The ultimate depth of high-resolution pulsed imaging depends on the optical parameters of a medium such as the refractive index n, scattering (μ_s) and absorption (μ_a) coefficients, and the scattering phase function $p(\theta)$, which is characterised by the average scattering cosine or the anisotropy factor g. The prediction of the ultimate depth of informative probing is an important problem. The solution of this problem, which should be based on the adequate models of interaction of pulsed radiation with a scattering medium, will reveal the possibilities of diagnostics of biological tissues by femtosecond pulses.

The propagation of light in an optically inhomogeneous medium is described by the integro-differential radiation transfer equation (RTE) [4, 5], which has no analytic solution in the general form. For this reason, the simplified forms of the RTE are studied which were obtained in different approximations and can be applied to describe the asymptotic regimes of the evolution of an optical beam in a scattering medium. The scattering of laser pulses was studied in detail analytically in the diffusion approximation [4, 6, 7], which is valid when the typical observation depth in the medium under study exceeds the transport length $l_{tr} = 1/(\mu_s' + \mu_a)$, where $\mu_s' = (1 - g)\mu_s$ is the reduced scattering coefficient. This condition means that the radiation field in the observation region is formed by photons multiply scattered by large angles. For a broad class of objects of biomedical diagnostics having a large anisotropy factor ($g \geqslant 0.9$), diffusion scattering is typical for depths exceeding several millimetres. In near-surface observation schemes with a high spectral resolution, on the contrary, a regime is realised in which a signal is mainly determined by the so-called snake photons which are scattered at a small angle in each scattering event during their propagation.

Such a regime is described in the small-angle RTE approximation [4, 8] assuming that the deviation angle θ of a photon from the beam axis is small, so that $\sin\theta \approx \theta$ and $\cos\theta \approx 1$. However, the study of the role of small-angle scattering in the propagation of light pulses should take into account the delay of scattered photons with respect to unscattered ones in the case of their deviation from a linear trajectory, which distorts the pulse shape. The elongation of the trajectory of a scattered photon in the small-angle

E.A. Sergeeva Institute of Applied Physics, Russian Academy of Sciences, ul. Ul'yanova 46, 603950 Nizhnii Novgorod, Russia; e-mail: sea@ufp.appl.sci-nnov.ru;
M.Yu. Kirillin Department of Physics, M.V. Lomonosov Moscow State University, Vorob'evy gory, 119992 Moscow, Russia; present address: Department of Technology, Optoelectronics and Measurement Techniques Laboratory, University of Oulu, P.O. Box 4500, 90014 University of Oulu, Finland; e-mail: mkirillin@yandex.ru;
A.V. Priezzhev Department of Physics and International Laser Center, M.V. Lomonosov Moscow State University, Vorob'evy gory, 119992 Moscow, Russia; e-mail: avp2@mail.ru

Received 27 June 2006; revision received 21 September 2006
Kvantovaya Elektronika **36** (11) 1023 – 1031 (2006)
Translated by M.N. Sapozhnikov

approximation can be taken into account with the help of the quadratic addition in the expansion of trigonometric functions of the scattering angle [9–11]: $\sin\theta \approx \theta$, $\cos\theta \approx 1 - \theta^2/2$, which considerably complicates the solution of the problem. The analytic expression for the profile of a scattered pulse taking into account the scatter in the delay times of photons was obtained in [12] in the small-angle diffusion approximation [4], which can be used only if the thickness of a scattering layer is much greater than the photon mean free path [defined as $1/(\mu_s + \mu_a)$] but does not exceed the transport length. The first restriction makes this model unacceptable for the description of the pulse distortions caused by low-order scattering.

The alternative of the theoretical description of radiation scattering is the numerical Monte-Carlo (MC) method of statistical tests based on the repeated calculation of random trajectories of photons in a medium under study and subsequent generalisation of the results obtained [13, 14]. This method can be used in a broad range of observation depths and for an arbitrary spatiotemporal structure of probe radiation. Monte-Carlo simulations are often applied to study the propagation of short pulses in scattering media [15, 16]. A disadvantage of the method, restricting its applications for solving inverse problems, is a long calculation time determined by the thickness of the medium in photon mean free paths and by the number of calculated photon trajectories. However, this restriction becomes now less substantial due to the development of computers and an increase in the computational resources required for accumulation of the sufficient statistics of tests.

In this paper, we studied analytically the propagation of a femtosecond pulse in a scattering medium with optical parameters close to those of biological tissues. We proposed the original model to describe pulse scattering, which takes into account small-angle scattering of both low and high orders and, therefore, can be used in a broader range of scattering depths compared to the model based on the small-angle diffusion approximation. Analytic expressions were obtained for the time profile of the two first scattering orders of the delta pulse in a medium with a Gaussian phase function. The pulse scattering was also studied by the MC method. The role of contributions from different scattering orders and ballistic component to the formation of a pulse scattered forward is analysed based on numerical calculations. The results of numerical calculations are compared with the results of the proposed theoretical model. It is shown that within the framework of approximations made in the solution of the problem, the theoretical model well agrees with MC simulations and can be used to describe distortions of the shape of a short pulse caused by small-angle scattering in an optically inhomogeneous medium. The method of approximate solution of the transient RTE can be applied for solving a broad class of problems of the optics of dispersion media, in particular, atmospheric optics and optics of aqueous media.

2. Materials and methods

2.1 Theoretical model of propagation of an ultrashort pulse in a turbid medium

The proposed model of scattering of an ultrashort pulse is based on the expansion of the light filed in a finite series in scattering orders. Contributions from individual scattering orders were calculated recurrently based on the RTE taking into account the effects of multipath propagation [11]. The last term of the series describes a source of a multiply scattered component, which is calculated in the small-angle diffusion approximation. This method was proposed in [17] to find the self-similar solution of the stationary RTE in a medium with strongly anisotropic scattering. Such an approach allows one to describe correctly the change in the pulse shape due to small-angle scattering at depths smaller than 10 mean free paths and the formation of the specific 'depth' time profile of the pulse in the regime of multiple scattering.

Consider the propagation of a pulsed unidirectional beam of brightness $L(\boldsymbol{r}, \boldsymbol{n}, t)$* in a plane layer of a scattering medium of thickness z. The beam brightness at the medium boundary ($z = 0$) is specified by the expression $L_0(\boldsymbol{r}_\perp, \boldsymbol{n}, t) = WR(\boldsymbol{r}_\perp)\delta(\boldsymbol{n} - \boldsymbol{z}_0)\delta(t)$, where W is the total pulse energy, the function $R(\boldsymbol{r}_\perp)$ determines the transverse structure of the beam at the input to the medium, and $\boldsymbol{z}_0$ is the unit vector of the z axis. The unit vector $\boldsymbol{n} = \boldsymbol{n}_\perp + n_z\boldsymbol{z}_0$ specifies the direction of beams with respect to the z axis. In the case of predominant small-angle scattering, the characteristic transverse deviations of beams from the z axis are small ($|\boldsymbol{n}_\perp| \ll 1$). The difference of the longitudinal projection of the vector $\boldsymbol{n}$ from unity can be taken into account with the help of the expression $n_z \approx 1 - \boldsymbol{n}_\perp^2/2$. Under the assumptions made above, the transfer equation [4] for the brightness $L(\boldsymbol{r}_\perp, z, \boldsymbol{n}_\perp, t)$ at the depth z in a medium with small-angle scattering is written in the form [8]

$$\left[\frac{1}{v}\frac{\partial}{\partial t} + \boldsymbol{n}_\perp\nabla_\perp + \left(1 - \frac{\boldsymbol{n}_\perp^2}{2}\right)\frac{\partial}{\partial z} + \mu_s + \mu_a\right] L(\boldsymbol{r}_\perp, z, \boldsymbol{n}_\perp, t)$$

$$= \frac{\mu_s}{4\pi}\iint_\infty L(\boldsymbol{r}_\perp, z, \boldsymbol{n}'_\perp, t)p(\boldsymbol{n}'_\perp, \boldsymbol{n}_\perp)\mathrm{d}^2\boldsymbol{n}'_\perp, \qquad (1)$$

where v is the speed of light in the medium, and the narrow scattering phase function depends on the angle between the directions of the beam before ($\boldsymbol{n}'$) and after ($\boldsymbol{n}$) scattering: $p(\boldsymbol{n}'_\perp, \boldsymbol{n}_\perp) = p(|\boldsymbol{n}'_\perp - \boldsymbol{n}_\perp|)$. It is convenient to use the spectral form of the RTE:

$$\left[\frac{\mathrm{i}\omega}{v} + \boldsymbol{n}_\perp\nabla_\perp + \left(1 - \frac{\boldsymbol{n}_\perp^2}{2}\right)\frac{\partial}{\partial z} + \mu_s + \mu_a\right] L^\omega(\boldsymbol{r}_\perp, z, \boldsymbol{n}_\perp)$$

$$= \frac{\mu_s}{4\pi}\iint_\infty L^\omega(\boldsymbol{r}_\perp, z, \boldsymbol{n}'_\perp)p(\boldsymbol{n}'_\perp, \boldsymbol{n}_\perp)\mathrm{d}^2\boldsymbol{n}'_\perp, \qquad (2)$$

where

$$L^\omega(\boldsymbol{r}_\perp, z, \boldsymbol{n}_\perp) = \frac{1}{2\pi}\int_{-\infty}^{\infty} L(\boldsymbol{r}_\perp, z, \boldsymbol{n}_\perp, t)\exp(\mathrm{i}\omega t)\mathrm{d}t$$

is the spectral brightness satisfying the boundary condition $L^\omega(\boldsymbol{r}_\perp, z = 0, \boldsymbol{n}_\perp) = WR(\boldsymbol{r}_\perp)\delta(\boldsymbol{n}_\perp)/2\pi$. Note that the form of Eqn (2) is similar to the stationary RTE in a medium with the effective absorption coefficient $\tilde{\mu}_a = \mu_a + \mathrm{i}\omega/v$ and effective attenuation coefficient $\tilde{\mu}_t = \tilde{\mu}_a + \mu_s = \mu_t + \mathrm{i}\omega/v$.

The distortion of a short pulse propagated through a plane scattering layer of thickness z is determined from the

*In the radiation transfer theory, along with the term 'brightness', the term 'radiation intensity' is also used, which is defined as the radiation flux per unit area per unit solid angle [18].

profile of the transmitted signal power. We will assume that radiation leaving the medium is detected with a detector with the Gaussian receiving diagram $D(\boldsymbol{n}) = \exp[-(\boldsymbol{n} - \boldsymbol{z}_0)^2/\Omega_0]$ having a maximum in the direction of the z axis and the spatial aperture of size greatly exceeding the characteristic spread of the beam caused by scattering. The width of the directivity diagram of the detector is characterised by the solid angle $\pi\Omega_0 = \int_{n_z \geqslant 0} D(\boldsymbol{n})\mathrm{d}\Omega_{\boldsymbol{n}}$. The quantity Ω_0 corresponding to the 'dispersion' of the receiving diagram is assumed small compared to the dispersion of the scattering angle $\langle\gamma^2\rangle$ ($\Omega_0 \ll \langle\gamma^2\rangle$). The received power is related to the brightness of radiation emerging from a layer of thickness z by the expression

$$P^{\omega}(z) = \iint_{\infty} \mathrm{d}^2\boldsymbol{r}_{\perp} \int_{n_z \geqslant 0} D(\boldsymbol{n}) L^{\omega}(\boldsymbol{r}_{\perp}, z, \boldsymbol{n}_{\perp}) \mathrm{d}\Omega_{\boldsymbol{n}}$$

$$\simeq \iint_{\infty} \mathrm{d}^2\boldsymbol{r}_{\perp} \iint_{\infty} L^{\omega}(\boldsymbol{r}_{\perp}, z, \boldsymbol{n}_{\perp}) \exp\left(-\frac{\boldsymbol{n}_{\perp}^2}{\Omega_0}\right) \mathrm{d}^2\boldsymbol{n}_{\perp},$$

from which it follows that for the detector geometry proposed above the spatial distribution of scattered radiation on the aperture is insignificant. In this case, it is convenient to introduce the integral characteristic

$$I^{\omega}(z, \boldsymbol{n}_{\perp}) = \iint_{\infty} L^{\omega}(\boldsymbol{r}_{\perp}, z, \boldsymbol{n}_{\perp}) \mathrm{d}^2\boldsymbol{r}_{\perp}$$

describing the angular structure of scattered light in the medium in an arbitrary section $z = \text{const}$. The power of the scattered signal measured with a detector with the receiving solid angle $\pi\Omega_0$ is determined by the integral from the angular distribution of radiation $I^{\omega}(z, \boldsymbol{n}_{\perp})$ taking into account the receiving diagram:

$$P^{\omega}(z) = \iint_{\infty} I^{\omega}(z, \boldsymbol{n}_{\perp}) \exp\left(-\frac{\boldsymbol{n}_{\perp}^2}{\Omega_0}\right) \mathrm{d}^2\boldsymbol{n}_{\perp}. \tag{3}$$

The time profile of the scattered pulse can be reconstructed by the inverse Fourier transform of the spectral power

$$P(z, t) = \int_{-\infty}^{\infty} P^{\omega}(z) \exp(\mathrm{i}\omega t) \mathrm{d}\omega. \tag{4}$$

The angular distribution of scattered light can be obtained from the stationary RTE with the effective attenuation index taking into account the multipath propagation of light and independent of the transverse coordinates:

$$\left[\left(1 - \frac{\boldsymbol{n}_{\perp}^2}{2}\right)\frac{\partial}{\partial z} + \tilde{\mu}_{\mathrm{t}}\right] I^{\omega}(z, \boldsymbol{n}_{\perp})$$

$$= \frac{\mu_{\mathrm{s}}}{4\pi} \iint_{\infty} I^{\omega}(z, \boldsymbol{n}'_{\perp}) p(\boldsymbol{n}'_{\perp}, \boldsymbol{n}_{\perp}) \mathrm{d}^2\boldsymbol{n}'_{\perp}. \tag{5}$$

Equation (5) describes in the corpuscular treatment a change in the distribution of photons over coordinates and propagation directions due to absorption and scattering [19], and the function $p(\boldsymbol{n}'_{\perp}, \boldsymbol{n}_{\perp})$ represents the probability density distribution for photon scattering from the direction $\boldsymbol{n}'$ to the direction $\boldsymbol{n}$. The factor $(1 - \boldsymbol{n}_{\perp}^2/2)$ in front of the derivative with respect to the longitudinal coordinate causes the spread of a pulse due to the multipath propagation of light [20]. The solution of Eqn (5) can be represented as an infinite series in the powers of the dimensionless parameter $\Lambda = \mu_{\mathrm{s}}/\mu_{\mathrm{t}}$ (Neumann series), which corresponds to the expansion in radiation scattering orders [21]. In this paper, we will seek the distribution $I^{\omega}(z, \boldsymbol{n}_{\perp})$ in the form of a finite series in scattering orders by assigning higher scattering orders to the multiply scattered ('diffusion') component [17]:

$$I^{\omega}(z, \boldsymbol{n}_{\perp}) = I_{\mathrm{b}}^{\omega}(z, \boldsymbol{n}_{\perp}) + \sum_{i=1}^{N} I_i^{\omega}(z, \boldsymbol{n}\perp) + I_{\mathrm{d}}^{\omega}(z, \boldsymbol{n}_{\perp}). \tag{6}$$

Here, I_{b}^{ω} is the brightness of unscattered radiation (which is formed by ballistic photons and is known as the first approximation of the multiple scattering theory); I_i^{ω} is the brightness of scattering of the ith order; I_{d}^{ω} is the brightness of light multiply scattered by a small angle. The brightness of unscattered light can be found from the Beer–Lambert law taking into account the boundary condition

$$I_{\mathrm{b}}^{\omega}(z, \boldsymbol{n}_{\perp}) = \frac{W \exp(-\tilde{\mu}_{\mathrm{t}} z)}{2\pi} \delta(\boldsymbol{n}_{\perp}),$$

which leads to the obvious expression

$$P_{\mathrm{b}}(t) = \frac{v}{z} W \exp(-\mu_{\mathrm{t}} z) \delta\left(\frac{vt}{z} - 1\right) \tag{7}$$

for the power of the unscattered component of the pulse.

The angular distribution of the ith-order scattering ($i = 1, \ldots, N$) satisfies the truncated RTE with the zero boundary condition and a source in the right-hand side formed by the $(i-1)$ component of scattered radiation

$$\left[\left(1 - \frac{\boldsymbol{n}_{\perp}^2}{2}\right)\frac{\partial}{\partial z} + \tilde{\mu}_{\mathrm{t}}\right] I_i^{\omega}(z, \boldsymbol{n}_{\perp}) = Q_i^{\omega}(z, \boldsymbol{n}_{\perp}),$$

$$Q_i^{\omega}(z, \boldsymbol{n}_{\perp}) = \frac{\mu_{\mathrm{s}}}{4\pi} \iint_{\infty} I_{i-1}^{\omega}(z, \boldsymbol{n}'_{\perp}) p(\boldsymbol{n}'_{\perp}, \boldsymbol{n}_{\perp}) \mathrm{d}^2\boldsymbol{n}'_{\perp}. \tag{8}$$

These relations allow one to obtain expressions for any scattering order in the small-angle approximation with the help of the iteration expression by integrating the density of sources along the propagation path of length $\xi_0 = z/n_z \simeq z(1 + \boldsymbol{n}_{\perp}^2/2)$:

$$I_i^{\omega}(z, \boldsymbol{n}_{\perp}) = \int_0^{\xi_0} \exp(-\tilde{\mu}_{\mathrm{t}}\xi) Q_i^{\omega}(z - n_z\xi, \boldsymbol{n}_{\perp}) \mathrm{d}\xi \quad (i = 1, \ldots, N). \tag{9}$$

The last term in sum (6), the multiply scattered component I_{d}^{ω}, can be found from the RTE with a distributed source whose density is determined by the brightness of light that has experienced N small-angle scatterings. We will calculate I_{d}^{ω} by using the RTE in the small-angle diffusion approximation [4], which is valid when the dispersion of the angular distribution of brightness is large compared to $\langle\gamma^2\rangle$:

$$\left[\left(1 - \frac{\boldsymbol{n}_{\perp}^2}{2}\right)\frac{\partial}{\partial z} + \tilde{\mu}_{\mathrm{a}} - \frac{1}{4}\mu_{\mathrm{s}}\langle\gamma^2\rangle\Delta_{\boldsymbol{n}_{\perp}}\right] I_{\mathrm{d}}^{\omega}(z, \boldsymbol{n}_{\perp}) = Q_{\mathrm{d}}^{\omega}(z, \boldsymbol{n}_{\perp}), \tag{10}$$

$$Q_{\mathrm{d}}^{\omega}(z, \boldsymbol{n}_{\perp}) = \frac{\mu_{\mathrm{s}}}{4\pi} \iint_{\infty} I_N^{\omega}(z, \boldsymbol{n}'_{\perp}) p(\boldsymbol{n}'_{\perp}, \boldsymbol{n}_{\perp}) \mathrm{d}^2\boldsymbol{n}'_{\perp}. \tag{11}$$

The method of solving the RTE in the small-angle diffusion approximation with a source distributed over the depth is described in [22] and is as follows. If the radiation distribution of the source is described by a Gaussian

$$Q_{\rm d}^{\omega}(z,\boldsymbol{n}_{\perp}) = \frac{P_{\rm s}^{\omega}}{\pi\Omega_{\rm s}^{\omega}}\exp\left(-\frac{\boldsymbol{n}_{\perp}^2}{\Omega_{\rm s}^{\omega}}\right), \tag{12}$$

and its power $P_{\rm s}^{\omega}$ and angular diagram $\pi\Omega_{\rm s}^{\omega}$ are functions of the medium thickness z, the detected power $P_{\rm d}^{\omega}$ of multiply scattered radiation can be represented in the form of the one-dimensional integral

$$P_{\rm d}^{\omega} = \Omega_0\int_0^z P_{\rm s}^{\omega}(z-z')\exp(-\tilde{\mu}_{\rm a}z){\rm d}z'$$

$$\times\left\{\left[\Omega_{\rm s}^{\omega}(z-z')+\Omega_0\right]\cosh(\tilde{\beta}z')\right.$$

$$\left.+\left[\frac{2\tilde{\beta}}{\tilde{\mu}_{\rm a}}+\frac{\tilde{\mu}_{\rm a}\Omega_0\Omega_{\rm s}^{\omega}(z-z')}{2\tilde{\beta}}\right]\sinh(\tilde{\beta}z')\right\}^{-1}, \tag{13}$$

where $\tilde{\beta} = (\tilde{\mu}_{\rm a}\mu_{\rm s}\langle\gamma^2\rangle/2)^{1/2}$.

The iteration procedure (8) allows one to obtain analytic expressions for the contributions of the first scattering orders if the phase function has the form convenient for integration. The simplest form of the small-angle phase function giving the analytic solution is the Gaussian distribution with the dispersion $\langle\gamma^2\rangle$ [4]:

$$p(\boldsymbol{n}'_{\perp},\boldsymbol{n}_{\perp}) = \frac{4}{\langle\gamma^2\rangle}\exp\left[-\frac{(\boldsymbol{n}_{\perp}-\boldsymbol{n}'_{\perp})^2}{\langle\gamma^2\rangle}\right]. \tag{14}$$

By using this function satisfying the normalisation condition

$$\frac{1}{4\pi}\iint_{\infty}p(\boldsymbol{n}'_{\perp},\boldsymbol{n}_{\perp}){\rm d}^2\boldsymbol{n}_{\perp} = 1,$$

the time distributions of singly and doubly scattered photons are represented in the form of tabulated integrals. Taking into account relations (3) and (4), the time profiles of the radiation power of the first two scattering orders (as functions of the relative delay $\tau = vt/z - 1$) have the form

$$P_1(\tau) = \frac{2v}{z}\,\frac{\mu_{\rm s}z}{\langle\gamma^2\rangle}\,W\exp[-\mu_{\rm t}z(1+\tau)]$$

$$\times\int_{2\tau[(\Omega_0+\langle\gamma^2\rangle)/\Omega_0\langle\gamma^2\rangle]}^{\infty}\frac{\exp(-x)}{x}{\rm d}x, \tag{15}$$

$$P_2(\tau) \simeq \frac{2v}{z}\left(\frac{\mu_{\rm s}z}{\langle\gamma^2\rangle}\right)^2 W\Omega_0\exp[-\mu_{\rm t}z(1+\tau)]$$

$$\times\int_{4\tau/\langle\gamma^2\rangle}^{\infty}\frac{\exp(-x)}{x^2}\left(x-\frac{4\tau}{\langle\gamma^2\rangle}\right){\rm d}x. \tag{16}$$

Figure 1 presents typical time profiles calculated for the ballistic component and components of singly, doubly, and multiply scattered radiation. One can see that singly scattered photons detected with a detector with a narrow receiving diagram do not distort considerably the delta pulse because they weakly deviate from a linear trajectory after scattering. At the same time, photons that have changed twice the direction of their propagation can acquire a considerable delay with respect to unscattered photons, which is manifested in the elongation of the trailing edge of the pulse. The influence of doubly scattered photons on the pulse shape is most considerable when the layer thickness is equal approximately to two mean free paths of photons in the medium. As the layer thickness increases, the role of higher-order scatterings in the distortion of the pulse shape also increases. The analytic calculation of high-order scatterings is quite time-consuming, and the solution is represented in the form of multiple integrals. Therefore, we will restrict in further calculations the series in expression (6) to two terms and will assume that the scattered pulse is described by four terms: $I^{\omega} = I_{\rm b}^{\omega} + I_1^{\omega} + I_2^{\omega} + I_{\rm d}^{\omega}$. In this case, the pulse power can be calculated from the expression

$$P = P_{\rm b} + P_1 + P_2 + P_{\rm d}. \tag{17}$$

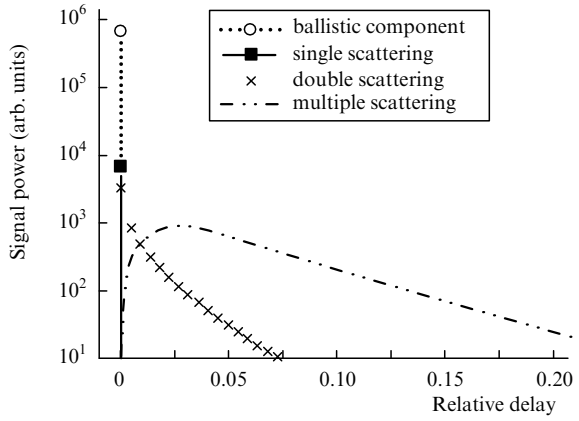

Figure 1. Typical analytic distributions of the relative delay times $\tau = vt/z - 1$ of photons of different scattering orders after the propagation of the delta pulse through an nonabsorbing layer of thickness $\mu_{\rm s}z = 10$ with the Gaussian phase function ($\langle\gamma^2\rangle = 0.2$).

In this approximation, photons scattered by more than two times are treated as 'diffusion' photons, and the source of the 'diffusion' component is doubly scattered photons:

$$Q_{\rm d}^{\omega}(z,\boldsymbol{n}_{\perp}) = \frac{\mu_{\rm s}}{4\pi}\iint_{\infty}I_2^{\omega}(z,\boldsymbol{n}'_{\perp})p(\boldsymbol{n}'_{\perp},\boldsymbol{n}_{\perp}){\rm d}^2\boldsymbol{n}'_{\perp}$$

$$= 2\left(\frac{\mu_{\rm s}}{\tilde{\mu}_{\rm t}\langle\gamma^2\rangle}\right)^3\frac{W\tilde{\mu}_{\rm t}\exp(-\tilde{\mu}_{\rm t}z)}{\pi^2}\int_0^{\tilde{\mu}_{\rm t}\langle\gamma^2\rangle z/2}{\rm d}\xi$$

$$\times\int_0^{\tilde{\mu}_{\rm t}\langle\gamma^2\rangle(z-\xi)/2}\exp\left[-\frac{\boldsymbol{n}_{\perp}^2}{\langle\gamma^2\rangle}\,\frac{(\xi+1)(\eta+2)-1}{(\xi+2)(\eta+2)-1}\right]$$

$$\times[(\xi+2)(\eta+2)-1]^{-1}{\rm d}\eta. \tag{18}$$

This relation cannot be further analytically simplified; however, the numerical calculation shows that it can be approximated by a Gaussian of type (12) whose parameters $P_{\rm s}^{\omega}$ and $\Omega_{\rm s}^{\omega}$ are calculated as the zero and second moments

of the angular distribution (18), respectively. The moments are expressed in the form of single integrals. The analytic approximations of these expressions which were used to calculate the profile of the 'diffusion' component of the pulse have the form

$$P_s^{\omega}(z) \simeq \frac{2W\mu_s^3 \exp(-\tilde{\mu}_t z)}{\pi\langle\gamma^2\rangle^2\tilde{\mu}_t^2} \ln\left(\frac{\tilde{\mu}_t\langle\gamma^2\rangle z}{8}+1\right) \ln\left(\tilde{\mu}_t\langle\gamma^2\rangle z+1\right),$$

$$\Omega_s^{\omega}(z) \simeq \langle\gamma^2\rangle \frac{\ln\left(\tilde{\mu}_t\langle\gamma^2\rangle z+1\right)}{\ln\left(\tilde{\mu}_t\langle\gamma^2\rangle z/3+1\right)}. \quad (19)$$

By substituting (19) into (13) and (4) and taking into account the replacements $\tilde{\mu}_a = \mu_a + i\omega/v$ and $\tilde{\mu}_t = \mu_t + i\omega/v$, we obtain the required expression for the time distribution of multiply scattered photons.

2.2 Monte-Carlo simulation of the scattered pulse structure

2.2.1. Scheme of the numerical experiment. As mentioned above, the MC method is based on repeated calculations of a random walk of photons in a scattering medium. Photon trajectories are simulated by using the input parameters μ_a and μ_s of the medium, the scattering phase function of inhomogeneities, and the geometry of the medium, incident beam, and detector. An advantage of numerical simulation of the photon trajectory in a scattering medium is the possibility of separation of detected photons in scattering orders, which is almost impossible to do experimentally [23]. This allows one not only to compare the analytically obtained distribution of photons over their propagation times in the medium with the results of MC simulations but also to compare contributions of each scattering orders under study.

We simulated the propagation of a Gaussian pulse of duration 50 fs (at the 1/e level) in a scattering layer of thickness 1 mm. Simulations were performed by using the MC algorithm developed and tested in papers [24, 25] with the statistics including 50 millions of photons. To obtain the correspondence between the conditions of the numerical experiment and the assumptions of the theoretical model, we assumed that a beam is incident on the medium surface perpendicular to the layer surface. An extended detector is located on the rear boundary of the medium and detects photons emerging from the medium at angles no more than one degree (which corresponds to $\Omega_0 = 3 \times 10^{-4}$) to the normal to the medium boundary. Depending on the optical parameters of the medium, one computer calculation took from 4 to 10 hours (2.4-GHz Pentium 4). The time resolution equal to 10 fs was determined by the optimal relation between the smoothness and the required calculation time.

2.2.2. Parameters of model media. The optical properties of the model medium were selected in accordance with the typical parameters of biological media and their phantoms in the wavelength range from 800 to 1300 nm. Because the optical characteristics of the medium in this spectral range weakly depend on the wavelength, we did not consider dispersion effects during the propagation of a femtosecond pulse with a rather broad spectrum. In addition, we neglected the influence of absorption on the pulse shape because the chosen spectral range corresponds to the transparency window of biological media where scattering greatly exceeds absorption.

Monte-Carlo simulations of pulse scattering and corresponding theoretical calculations were performed for three values of the scattering coefficient $\mu_s = 5$, 10, and 20 mm^{-1} and for two values of the anisotropy factor $g = 0.9$ and 0.98 specified for each scattering coefficient. By combining these parameters in pairs, we simulated different scattering regimes: from the 'quasi-ballistic' regime, in which low-order scatterings dominate, to the 'quasi-diffusion' regime in which small-angle multiple scattering of photons plays a main role. When the anisotropy factor is close to unity, the dispersion of the scattering angle $\langle\gamma^2\rangle$ can be expressed in terms of g by the relation $g \simeq 1 - \langle\gamma^2\rangle/2$. For the anisotropy factor equal to 0.9 and 0.98, the dispersion of the scattering angle was 0.2 and 0.04, respectively. The solid receiving angle was specified to satisfy the condition $\Omega_0 \ll \langle\gamma^2\rangle$.

It is important to note that the distortion of the pulse profile depends not only on the value of g but the shape of the scattering phase function itself. To demonstrate this fact, we considered two phase functions of different shapes but corresponding to the same anisotropy factor. The first function is the Gaussian phase function (14) for which the dispersion of a random scattering angle is unambiguously determined from the value of g [7]. This function allows one to calculate analytically the scattered pulse profile and compare it with the MC simulation. A disadvantage of calculations based on this function is that they give a very weak scattering into the rear hemisphere. For this reason, scattering in real media is sometimes described by approximating the phase function by the sum of a Gaussian and a constant [26]. However, in the small-angle scattering approximation and for the chosen values of the anisotropy factor, the contribution of the Gaussian component to the total phase function dominates. The second function is the Henyey–Greenstein phase function

$$p(\theta) = \frac{1}{2}\frac{1-g^2}{(1+g^2-2g\cos\theta)^{3/2}}$$

which is widely used in MC simulations of the propagation of light in biological tissues [1].

Figure 2 presents these two phase functions for scattering angles in the range from 0 to 90° (functions are normalised to the integral over the total solid angle). One can see that for the same anisotropy factor, the Henyey–Greenstein function is more elongated forward than the Gaussian phase function, which affects the group delay of the signal. Unfortunately, the iteration problem of calculating the contributions of the first scattering orders cannot be solved analytically by using (8) with the Henyey–Greenstein function. Therefore, the results of the theory and simulations were not compared for this phase function.

3. Results and discussion

To verify the developed analytic model of pulse scattering and determine the region of its applications, we compared theoretical calculations with MC simulations of the profile of a 50-fs pulse scattered in a layer of thickness 1 mm and recorded with an extended detector with the diagram $\pi\Omega_0 = 9.7 \times 10^{-3}$ sr. The contributions of the ballistic component, the first two scattering orders, and multiple scattering to the pulse were calculated from relations (7), (13), (15), (16), and (19) for Gaussian function (14). Monte-Carlo simulations were performed for the same parameters

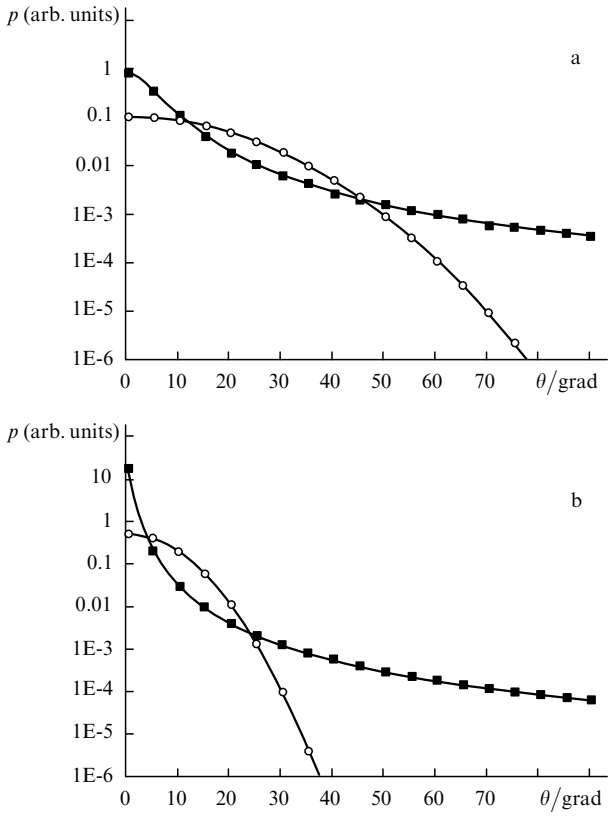

Figure 2. Henyey–Greenstein (■) and Gaussian (○) phase functions $p(\theta)$ with the anisotropy factor 0.9 (a) and 0.98 (b).

of the medium. The calculated and simulated results were normalised by matching energies stored in ballistic components.

For convenience, we present first the results of MC simulations.

3.1 Influence of optical parameters on the scattered pulse shape: MC simulations

The structure of a scattered pulse is determined by contributions from photons that have experienced different numbers of scattering events. In turn, there exists a spread in the delay times of photons scattered by a certain number of times. The relation between contributions from different scattering orders to the detected signal, as the distribution of photons in their paths within one scattering order, considerably depends on the characteristics of a scattering event such as the phase function and scattering coefficient. To demonstrate this, we performed MC simulations of the profile of a 50-fs pulse scattered forward in a layer of thickness 1 mm and studied the distribution of the arrival times of singly, doubly, triply, and multiply scattered photons. We investigated the influence of the following factors: (i) the degree of anisotropy of the phase function of the specified shape for the invariable scattering coefficient; (ii) the scattering coefficient of the medium for the specified phase function; and (iii) the phase function shape for invariable values of the anisotropy factor and scattering coefficient.

The results of calculations of the pulse profile are presented in Figs 3–5. On the abscissa in all the figures the arrival time (in picoseconds) of photons to the detector measured from the instant of entrance of the pulse maximum to the medium is plotted. Figure 3 shows the time distributions of photons with different scattering orders for a medium with the Henyey–Greenstein phase function, the anisotropy factors $g = 0.98$ and 0.9, and the scattering coefficient $\mu_s = 10$ mm^{-1}. Detection is performed with a detector with a narrow angular diagram. It is obvious that the absolute contribution of the ballistic component to the pulse is the same for both values of g because its intensity depends only on the scattering coefficient but not on the anisotropy factor of the medium. However, the relative contribution of the ballistic component proves to be higher for $g = 0.9$ because at lower values of g the phase function is less elongated forward and a greater part of scattered photons is 'filtered out' by a small detection angle. For the case $g = 0.98$, which is characterised by smaller scattering angles of photons, the contribution of low-order scatterings exceeds the contribution of the ballistic component (for the specified scattering coefficient). A smaller anisotropy factor results in greater scattering angles of photons, which is manifested in the formation of a slowly decaying trailing edge of the pulse caused by long delay times of scattered photons.

Figure 4 illustrates the influence of the scattering coefficient on the pulse shape. Pulse profiles are presented for three values of the scattering coefficient of the medium with the Henyey–Greenstein phase function and the anisotropy factor equal to 0.98. As the scattering coefficient increases,

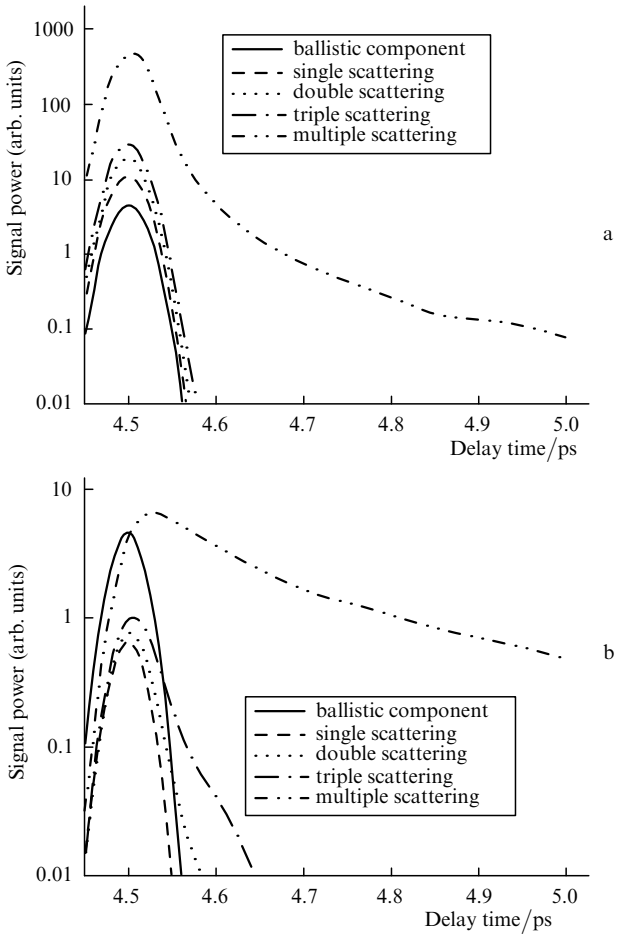

Figure 3. Contributions of photons of different scattering orders to the propagated pulse for a medium with $\mu_s = 10$ mm^{-1} and the Henyey–Greenstein phase function for $g = 0.98$ (a) and 0.9 (b).

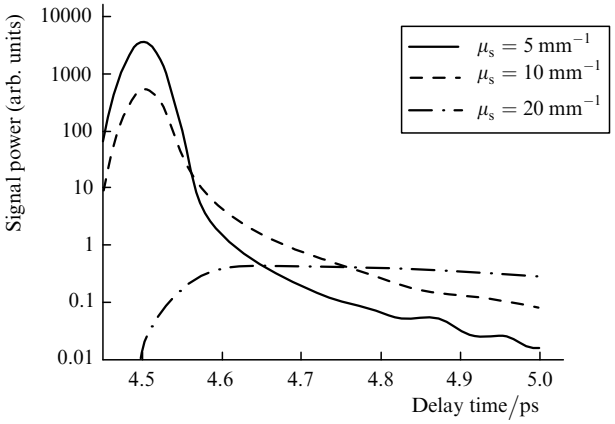

Figure 4. Shape of the pulse propagated through a scattering medium (the Henyey–Greenstein phase function, $g = 0.98$) for different scattering coefficients μ_s.

the ballistic component forming the front power peak delayed by 4.5 ps decreases and its energy is transferred to scattered photons. The intensity of the trailing edge of the pulse increases due to multiple scattering forming a signal in the region of large delays. For $\mu_s = 20$ mm^{-1}, the power maximum shifts to longer delays, which suggests that multiply scattered photons dominate in the signal.

Figure 5 presents the integrated contributions of all components under study to the pulse for different values of the scattering coefficient and anisotropy factor calculated for a medium with the Henyey–Greenstein phase function. One can see that, as the scattering coefficient increases, the fraction of ballistic photons and photons of lower scattering orders decreases for both values of the anisotropy factor, while the fraction of photons of higher scattering orders increases. This is explained by the increase in the average number of scattering events experienced by photons propagating through the layer. In addition, for any specified value of μ_s, the fraction of ballistic photons for a lower anisotropy factor ($g = 0.9$) exceeds the fraction of ballistic photons for a higher anisotropy factor. This, as mentioned above, is explained by the peculiarity of the problem geometry and is related to a high angular selectivity of the detector.

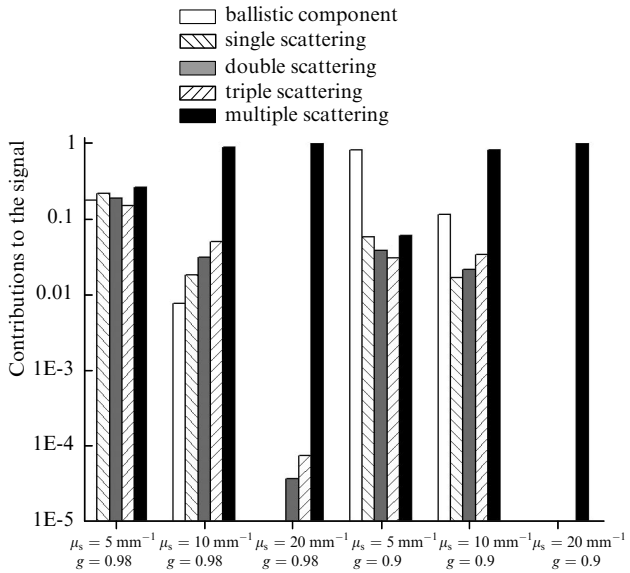

Figure 5. Relative contributions of photons of different scattering orders to the pulse scattered forward for different optical parameters of the medium.

The influence of the shape of the scattering phase function on the time structure of the pulse is illustrated in Fig. 6 where the pulse profiles are presented for media with phase functions of two types and $\mu_s = 10$ mm^{-1} and $g = 0.9$. For these scattering parameters, the medium thickness is equal to one transport length, so that the light field near the detector is mainly formed by diffusively scattered photons. One can see from Fig. 6 that the structure of the scattered pulse is predominantly determined by the shape of the phase function even when the anisotropy factor remains constant. In a medium with the Henyey–Greenstein phase function, the energy of the scattered pulse is mainly contained in ballistic photons and photons arriving at a detector with a small delay (because the pulse peak corresponds to the arrival time of photons of the ballistic component with an error of the order of the time resolution of the detector equal to 10 fs); however, these photons are not necessarily photons of low orders of scattering. At the same time, in a medium with the Gaussian scattering function, the pulse is divided into two distinct fractions, of which the first one contains mainly ballistic photons, while the second one is formed by multiply scattered photons having large delays compared to the width of the initial pulse. Such a difference in the profiles of the scattered pulse is determined by the degree of forward elongation of the scattering function, i.e., by the relation between the probabilities of photon scattering near the zero direction and scattering by angles exceeding the mean angle. For the specified anisotropy factor, 50 % of light is scattered inside a cone with the cone angle 10° in the case of the Henyey–Greenstein phase function and 14 % in the case of the Gaussian function. This affects the delay times of photons forming the trailing edge of the pulse and gives rise to a gap between fractions in the profile of the pulse propagating in a medium with the Gaussian distribution function.

3.2 Comparison of the theoretical and numerical calculations of the scattered pulse structure

The shape of a scattered pulse of duration 50 fs in analytic calculations is determined by the time convolution of the Gaussian profile of the incident pulse with a specified

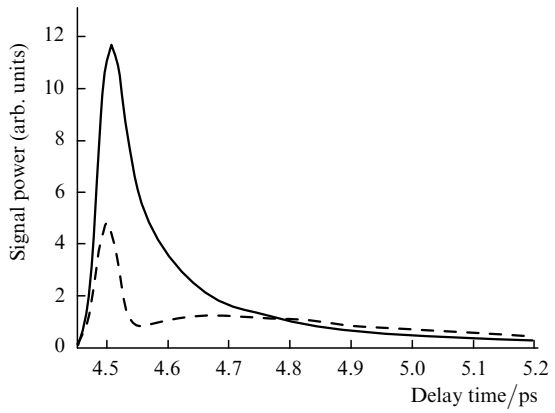

Figure 6. Pulse shapes at the output from the medium ($\mu_s = 10$ mm^{-1}, $g = 0.9$) for the Henyey–Greenstein (solid curve) and Gaussian (dashed curve) phase functions.

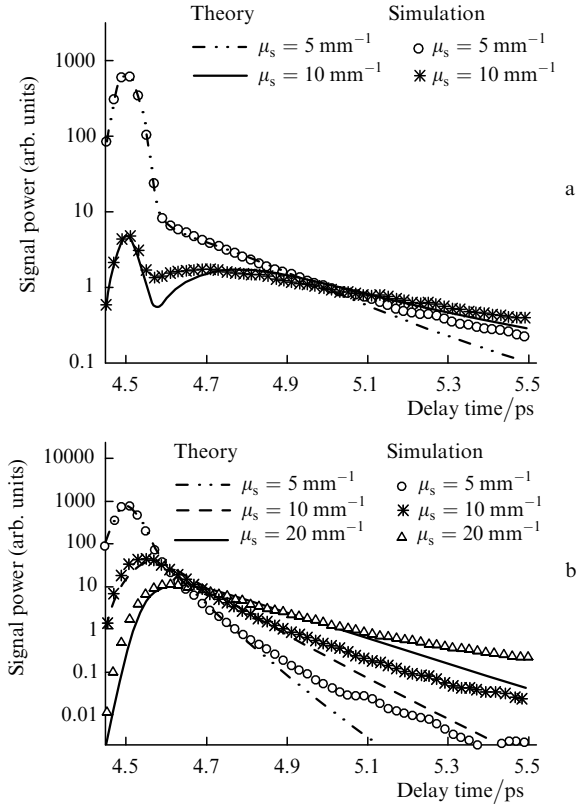

Figure 7. Profiles of the pulse propagated through a scattering medium calculated theoretically and numerically for the anisotropy factors of the Gaussian phase function $g = 0.9$ (a) and 0.98 (b).

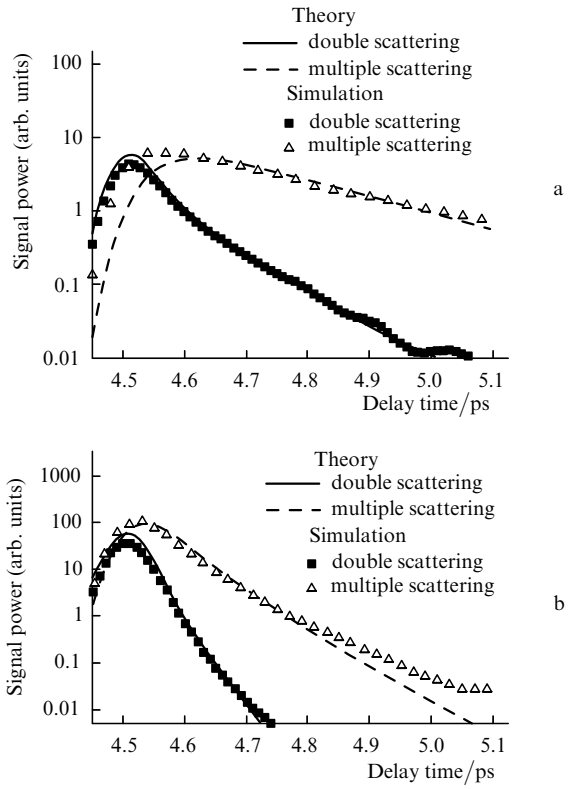

Figure 8. Comparison of contributions from photons of different scattering orders to the pulse propagated through a scattering medium [$\mu_s = 5$ mm^{-1}, Gaussian phase function, $g = 0.9$ (a) and 0.98 (b)] calculated theoretically and by the MC method.

energy and functions P_b, P_1, P_2, and P_d determining the contributions of corresponding scattering components of the input delta pulse with the unit energy $W = 1$. The profiles of a scattered pulse calculated by using the developed analytic model and MC simulations for two different anisotropic factors of the Gaussian phase function are presented in Fig. 7.

One can see from the figure that the theoretical model reflects adequately as a whole the main features of the scattered pulse and describes accurately enough the pulse shift and broadening. For all the proposed combinations of scattering parameters, except a medium with $\mu_s = 10$ mm^{-1} and g = 0.9, the model well agrees with the MC simulation for small time delays; however, the theory predicts the understated signal intensities for large delay times. This is obviously explained by the use of the small-angle scattering approximation in the theoretical model, which incorrectly considers strong deviations of photons from the longitudinal axis responsible for large delays. The maximum discrepancy between analytic calculations and MC simulations is observed for a medium with $\mu_s = 10$ mm^{-1} and $g = 0.9$; in this case, the theory predicts the insufficient number of scattered photons with the time delay on the order of the initial pulse duration. A similar feature is also observed in Fig. 8 where the contributions of doubly and multiply scattered photons to the scattered pulse are compared.

One can see that the partial contribution of doubly scattered photons can be calculated analytically with an acceptable accuracy for both values of the anisotropy parameter. However, when doubly scattered radiation is used as a source of multiply scattered photons, good agreement between the theoretical model and MC simulations is possible only in the case of a rather narrow scattering phase function. The reason is that the small-angle diffusion approximation used in the model is valid when $\mu_s(1 - g)z < 1$ [12], which corresponds to $g \geqslant 0.9$ for $\mu_s = 5$ mm^{-1} and $g \geqslant 0.95$ for $\mu_s = 10$ mm^{-1}. Figure 7 shows that for media with the anisotropy factor $g = 0.98$, the theory is in good agreement with numerical calculations for all selected values of the scattering coefficient. The discrepancy between theoretical and simulation results for $g = 0.98$ is probably caused by the fact that the small-angle diffusion approximation is invalid for a part of multiply scattered photons. It can be expected that this discrepancy will decrease if photons of higher scattering orders are used as a source of the diffusion component. Unfortunately, we failed to obtain an analytic expression for calculating the contribution of photons of scattering orders above the second order, even by using the Gaussian scattering phase function.

Note that this discrepancy between the theory and MC simulation is observed for the thickness of a scattering layer of the order of the transport length (for example, for a medium with $\mu_s = 10$ mm^{-1} and $g = 0.9$, the transport length is $l_t = 1$ mm), when other approximations should be used for solving the RTE. At the same time, the parameters of all media with $g = 0.98$ correspond to the regime of multiple, but 'prediffusion' scattering, i.e. the thickness of the media does not exceed the transport length. A comparison with the MC simulation also demonstrates that the proposed analytic solution can be also applied in the case of low-order scattering ($\mu_s z < 10$). Thus, the model containing the contributions of the ballistic component, the first two scattering orders, and multiply scattered component can be successfully used to describe the scattering of a

femtosecond pulse in a broader range of thicknesses of scattering layers than the region of applications of the small-angle diffusion approximation.

4. Conclusions

We have analysed theoretically and numerically the evolution of the profile of a femtosecond laser pulse propagating in a scattering medium and proposed the analytic model of scattering of an ultrashort pulse based on the calculation of contributions from photons of different scattering orders. The iteration calculation of the partial components of the pulse was performed by solving the radiation transfer equation taking into account the spread in the delay times of photons. In the case of the Gaussian scattering phase function, analytic expressions have been obtained for the contributions of singly and doubly scattered photons upon detection of radiation with an extended detector with a narrow angular diagram. The brightness of multiply scattered radiation was calculated in the small-angular approximation of the RTE with doubly scattered light as a distributed source. The proposed model is valid in the region of scattering parameters where other known approximations cannot be used. We also performed MC simulations of the scattered pulse structure by separating the ballistic component, singly, doubly, and multiply scattered photons. Numerical calculations have shown that the pulse shape strongly depends on the form of the scattering phase function with the anisotropy factor being preserved because the degree of elongation of the phase function determines the time delay of photons during small-angle scattering. We also have analysed quantitatively the fractions of different components in the scattered pulse depending on the optical properties of the medium. In the case of the Gaussian phase function, the profiles of the scattered pulse calculated theoretically and in MC simulations have been compared. It has been demonstrated that the analytic model of propagation of a femtosecond pulse in a scattering medium has a broader scope of applications and can be used to describe both quasi-ballistic and quasi-diffusion regimes of pulse scattering in an optically inhomogeneous medium.

Acknowledgements. The authors thank L.S. Dolin for useful discussions and comments during the preparation of the manuscript. This work was supported by the Russian Foundation for Basic Research (Grant Nos 04-02-17108, 04-02-16748, 06-02-17015), the GETA Graduate School, Finland, and also partially supported by Grants No. NSh 2071.2003.4 and No. NSh 6043.2006.2 of the President of the Russian Federation for the Support of Leading Scientific Schools in Russia.

References

1. Tuchin V.V. *Usp. Fiz. Nauk.*, **167**, 517 (1997).
2. Tuchin V.V. *Lasery i volokonnaya optika v biomeditsinskikh issledovaniyakh* (Lasers and Fibre Optics in Biomedical Studies) (Saratov: Saratov State University, 1998).
3. Vo-Dinh T. (Ed.) *Biomedical Photonics Handbook* (Boca Raton, FL: CRC Press, 2003).
4. Ishimaru A. *Wave Propagation and Scattering in Random Media* (New York: Academic Press, 1978; Moscow: Mir, 1981) Vols 1 and 2.
5. Mishchenko M.I., Travis L.D., Lacis A.A. *Multiple Scattering of Light by Particles: Radiative Transfer and Coherent Backscattering* (Cambridge: Cambridge University Press, 2006).
6. Zege E.P., Ivanov A.P., Katsev I.L. *Perenos izobrazheniya v rasseivayushchei srede* (Radiation Transfer in a Scattering Medium) (Minsk: Nauka i Tekhnika, 1985).
7. Winn J.N., Perelman L.T., Chen K., Wu J., Dasari R.R., Feld M.S. *Appl. Opt.*, **37**, 8085 (1998).
8. Kokhanovsky A.A. *J. Phys. D: Appl. Phys.*, **30**, 2837 (1997).
9. Dolin L.S. *Izv. Vyssh. Uchebn. Zaved., Ser. Radiofiz.*, **9**, 61 (1966).
10. Minin I.M. *Teoreticheskie i prikladnye problemy rasseyaniya sveta* (Theoretical and Applied Problems of Light Scattering) (Minsk: Nauka i Tekhnika, 1971).
11. Romanova L.M. *Nestatsionarnoe svetovoe pole v mutnykh sredakh* (Transient Light Field in Turbid Media) (Minsk: Nauka i Tekhnika, 1971).
12. Rogozkin D.B. *Izv. Akad. Nauk SSSR, Ser. Fiz. Atmos. Okean.*, **23**, 275 (1987).
13. Wang L., Jacques S.L., Zheng L. *Computer Methods and Progr. in Biomed.*, **47**, 131 (1995).
14. Kandidov V.P. *Usp. Fiz. Nauk.*, **166**, 1309 (1996).
15. Jacques S.L. *Appl. Opt.*, **28**, 2223 (1989).
16. Blanca C.M.Y., Saloma C. *Appl. Opt.*, **38**, 5433 (1999).
17. Dolin L.S. *Dokl. Akad. Nauk SSSR*, **260**, 1344 (1981).
18. Sobolev V.V. *Kurs teoreticheskoi astrofiziki* (Course of Theoretical Astrophysics) (Moscow: Nauka, 1967).
19. Apresyan L.A., Kravtsov Yu.A. *Teoriya perenosa izlucheniya* (Theory of Radiation Transfer) (Moscow: Nauka, 1983).
20. Furutsu K. *J. Math. Phys.*, **20**, 617 (1979).
21. Rytov S.M., Kravtsov Yu.A., Tatarskii V.I. *Statisticheskaya radiofizika, Ch. II, Sluchainye polya* (Statistical Radiophysics, Part II: Random Fields) (Moscow: Nauka, 1980).
22. Dolin L.S. *Izv. Vyssh. Uchebn. Zaved., Ser. Radiofiz.*, **26**, 300 (1983).
23. Wang R.K. *Phys. Med. Biol.*, **47**, 2281 (2002).
24. Kirillin M.Yu., Meglinski I.V., Priezzhev A.V. *Kvantovaya Elektron.*, **36**, 247 (2006) [*Quantum Electron.*, **36**, 247 (2006)].
25. Kirillin M.Yu., Priezzhev A.V., Tuchin V.V., Wang R.K., Myllyla R. *J. Phys. D: Appl. Phys.*, **38**, 2582 (2005).
26. Turchin I.V., Sergeeva E.A., Dolin L.S., Kamensky V.A. *Laser Phys.*, **13**, 1524 (2003).